Highly Specific and Wide Range NO_2 sensor with color readout.

Cristian Fàbrega[*,1,2], Luis Fernández[1], Oriol Monereo[1], Alba Pons-Balagué[1], Elena Xuriguera[2,3], Olga Casals[1,2], Andreas Waag[3,4] and Joan Daniel Prades[1,2].

[1]MIND-Departament of Electronics, Universitat de Barcelona (UB), c/Martí i Franquès 1, E-08028 Barcelona, Spain.

[2] Institute of Nanoscience and Nanotechnology (IN²UB), Universitat de Barcelona (UB), c/Martí i Franquès 1, E-08028 Barcelona, Spain.

[3]DIOPMA, Departament de Ciència de Materials i Química Física, Universitat de Barcelona, Spain.

[4]Institute of Semiconductor Technology, Braunschweig University of Technology, Germany.

[5]Laboratory for Emerging Nanometrology LENA, Braunschweig, Germany.

KEYWORDS: NO_2; sensor; colorimetry; Griess-Saltzman; pollutant; monitoring; environment;

ABSTRACT: We present a simple and inexpensive method to implement a Griess-Saltzman-type reaction that combines the advantages of the liquid phase method (high specificity and fast response time) with the benefits of a solid implementation (easy to handle). We demonstrate that the measurements can be carried out using conventional RGB sensors; circumventing all the limitations around the measurement of the samples with spectrometers. We also present a method to optimize the measurement protocol and target a specific range of NO_2 concentrations. We demonstrate that it is possible to measure the concentration of NO_2 from 50 ppb to 300 ppm with high specificity and without modifying the Griess-Saltzman reagent.

Nitrogen dioxide (NO_2) is an extremely toxic gas generated primarily as a byproduct of combustion processes such as car engines, power plants and cigarette smoke[1,2]. Moreover, it is believed to cause cancer due to its high reactivity with genetic material and organic solvents, forming nitrosamines[3]. Any form of nitrogen oxide (NO_x) at levels greater than 1 ppm can cause serious damage to human respiration systems and lung tissues. The small molecules can penetrate deeply into the sensitive parts of lungs causing or worsening of respiratory diseases such as emphysema and bronchitis or aggravate existing heart disease[4]. NO_2 is also a source of acid rain, damaging buildings and polluting water sources[5]. Thus, monitoring NO_2 is of paramount importance for making our environment safer and cleaner.

Measuring NO_2 is specially challenging because nitrogen species in pollutant and toxic emissions are specified as NO_x due to the diversity of possible nitrogen oxidation states. Also, due to its oxidizing character, its signal in sensors based on redox mechanisms is subjected to strong cross interferences with other oxidizing species, like oxygen or ozone. Furthermore, the range of concentrations at which it should be detected to trigger a safety alarm are very low (under 1 ppm).

As a result, the detection of NO_2 in gas phase with low cost sensors is a demanding task. Electrochemical sensors offer a good sensitivity and specificity towards this gas, but they are bulky, mostly based on liquid electrolytes and require frequent calibration[6]. Solid state sensors based on redox processes occurring on semiconductors, like metal oxides or carbon-based materials, are sensitive, relatively inexpensive, but quite unspecific, and demand a high-power budget to come into fast and reversible operation[7]. Finally, color-based methods offer good specificity but their quantitative readout is complex[8]. In safety industry, color-based solutions are gold standards to monitor specific compounds like NO_2 in the field, but these measurements are expensive, based on a consumable accompanied by a readout tool[9]. Therefore, a measurement method that could offer good sensitivity and specificity in a simple and cheap measurement format is lacking.

Different color-changing dyes to indicate the presence of NO_2 have been reported. In 1964, Saltzman[10] proposed a reagent consisting of a combination of sulphanilic acid and glacial acetic acid as absorbing reagent and *N*-(1-naphthyl)-etylenediamine dihydrochloride that turns from transparent to deep-purple in the presence of NO_2 in a non-reversible way. This reaction is extremely specific towards NO_2 and is in common use in analytical chemistry. In this field, it has been successfully used to monitor from 5 ppb to 300 ppm of NO_2, by bubbling the sample through the Saltzman reagent[11,12]. After exposing the reagent to the gas sample, the concentration of NO_2 ions is determined by analyzing the absorption spectra of the products using bulky and costly UV-visible spectrometers.

This wet methodology is complex, requires trained personnel and cannot be carried out in the field or in an automated way with inexpensive means.

Recently, several works reported on improvements of this approach. Izumi et al. suggested to deposit and dry the Saltzman reagents on top of porous silica substrates[13] coupled to a permanganate oxidizer to oxidize NO to NO_2. This was a handy, dry configuration, which proved that the color change also develops in solid state. However, the response time of these samples was extremely slow (more than 30 minutes to detect 5 ppm of NO_2), due to the low mobility of the reagents in the solid-dry matrix.

Here, we present a simple an inexpensive method to implement a Griess-Saltzman-type reaction that combines the advantages of the liquid phase method (high specificity, fast response time) with the benefits of a solid implementation (easy to handle, store, expose to gases and measure). We demonstrate that the measurements can be carried out using conventional RGB sensors, such as the ones found in smartphone cameras; circumventing all the limitations around the optical measurements with spectrometers. We also present a model of the reaction that can be used to optimize the measurement protocol and target a specific range of NO_2 concentrations. Applying this methodology, we demonstrate that it is possible to measure the concentration of NO_2 from 50 ppb to 300 ppm with high specificity and without modifying the sensing elements.

Experimental Section

The Griess-Saltzman (GS) reagent was prepared, according to the standarized method, by dissolving 5 grams of sulfanilic acid (reagent grade ACS crystals) in 940 ml of 2.5M acetic acid. After dissolution, 5 ml of a 1 % aqueous solution of N-(1-naphthy1)ethylenediamine dihydrochloride were added and the solution was diluted to volume in a 1-liter volumetric flask.

To fabricate the sensor elements (from now on, "sensor pads"), we soaked 2.5 cm x 2.5 cm x 0.3 cm squares of sterilized cellulose absorbent pads with 0.2 ml of the indicator solution. To assure an homogeneous impregnation of the reagent, the soaked pads were allowed tosettle for 8 hours in synthetic dry air before carrying out any experiment with them. To test their endurance, the pads were packaged in dry synthetic air in a gas tight plastic film enclosure and stored for up to 6 months, obtaining no significant differences with the results reported here.

Gas sensing experiments were conducted in a customized chamber of 15 ml in volume. Gas mixtures were introduced with thermal mass flow controllers (Bronkhorst HighTech-200 ml) by mixing dry synthetic air (SA) with NO_2 in SA from certified gas cylinders. A 10 ppm NO_2 in SA and a 300 ppm NO_2in SAcylinders were used for low and high concentration experiments, respectively. The interfering gases used were pureO_2, CH_4, C_2H_6O, CO, and NH_3diluted in SA from certified gas cylinders of 1% for CH_4 and 100 ppm for the rest. Humidity was introduced by bubbling SA through a water trap.

The spectral measurements were acquired with a UV-visible spectrometer (Specord 205, Analytik Jena) in an integrating sphere configuration using a customized sample holder to accommodate our wet pads. The samples were measured in less than 10 minutes after exposure to the gases, and were transported in a gas tight chamber containing dry synthetic air.

The color measurements were carried out in a homemade apparatus based on a TCS3200 RGB color sensor in combination with an illumination source made of 4 white LEDs. The sensor transforms the light intensity in each of the red, green and blue bands into 3 frequency-modulated square pulse signals. These 3 frequencies, rangingfrom 0 Hz (dark) to 120 kHz (maximum illumination), were acquired with 3 frequency counters implemented with an Atmel ATmega328P microcontroller. Before every measurement, the frequency signals were normalized to the value of a blank water-soaked sensor pad used as a reference, following a strategy similar to a white balance correction. In this way, 3 signals ranging from 0 to 1 were obtained. Black corresponded to [0,0,0], white to [1,1,1], and pure red/green/blue to [1,0,0]/[0,1,0]/[0,0,1], respectively. To guarantee the stability of the illumination conditions, the 4 white LEDs were allowedto stabilize for 3 hours before every round of measurements.

Results and Discussion

NO_2 hydrolyze in contact with water in the form of

$$2\,NO_2 + H_2O \xrightarrow{yields} HNO_2 + HNO_3 \qquad (1)$$

Then, only nitrite ions (NO_2^-) in water solution react with sulfanilic acid forming a diazonium salt, which further reacts with the naphthylamine component forming the azo dye (Figure 1).

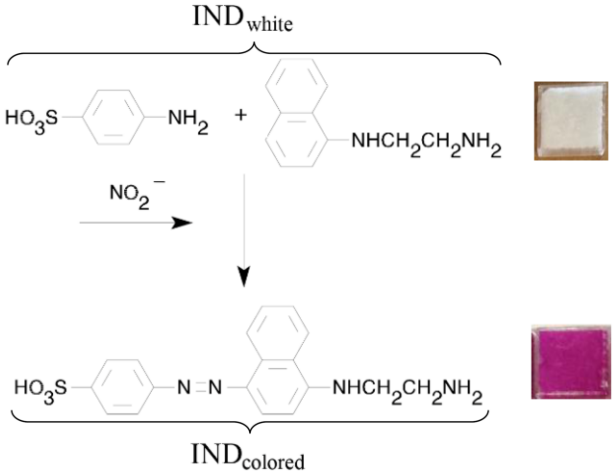

Figure 1. Scheme of the Griess-Saltzman reaction.

For simplicity, the overall reaction can be written as follows:

$$\begin{cases} 2NO_{2\,air} \rightarrow NO^-_{2\,liq} \\ NO^-_{2\,liq} + IND_{White} \rightarrow IND_{Colored} \end{cases} \quad (2)$$

where IND_{White} refers to the GS indicator solution (sulfanilic acid, glacial acetic acid, and naphthylamine) before any nitrite reaction event, and $IND_{Colored}$ refers to the same indicator solution after nitrite reaction.

Spectral Response

Upon exposure to NO_2, the sensor pads developed the expected deep-purple coloration of the GS indicator (Figure 2). To understand the origin of this color change, the pads were exposed to increasing concentrations of NO_2 ranging from 1 ppm to 300 ppm diluted in SA for 5 minutes. Immediately, their reflectance spectra were acquired obtaining the results presented in Figure 2. Besides some steady features in the infrared range, the spectra are dominated by an asymmetric absorption band centered around 540 nm that develops further with increasing concentrations of NO_2.

RGB Response

For the sake of simplicity, we chose to proceed in further experiments using a simplified spectral signal, corresponding to the red, green and blue range responses of a commercial RGB sensor.

In order to demonstrate that such RGB signals contain sufficient spectral information to study the color changes in the pads, we first simulated the RGB signals that we would obtain if an RGB sensor were used to measure the color spectra acquired in Figure 2.

The reflected color signal in each color channel of an RGB sensor can be calculated as:

$$\langle S \rangle = \frac{\int_{\lambda_{min}}^{\lambda_{max}} I(\lambda) \cdot R(\lambda) \cdot D(\lambda) d\lambda}{\int_{\lambda_{min}}^{\lambda_{max}} D(\lambda) d\lambda} \,, \quad (3)$$

where $\langle S \rangle$ stands for the signal in each of the R, G or B ranges (leading to ⟨R⟩, ⟨G⟩ and ⟨B⟩ respectively), $D(\lambda)$ is the spectral response of the detector used to acquire the ⟨R⟩, ⟨G⟩ or ⟨B⟩ signals, $I(\lambda)$ is the spectra of the incident light, and $R(\lambda)$ is the reflectance spectra of the pads. The integral runs for all the wavelengths in the range of interest. The denominator is a normalization factor that corresponds to the response of the sensor to a blank reference color, whose reflectance spectra is reconsidered 1 at all wavelengths. Thus, using eq.(3) it is possible to predict the RGB values acquired by the sensor; provided that the light source, the spectral response of the sensors, and the reflectance of the samples were known. From now on, all ⟨R⟩, ⟨G⟩ and ⟨B⟩ signals will be normalized to 1. Also, a mean signal value defined as

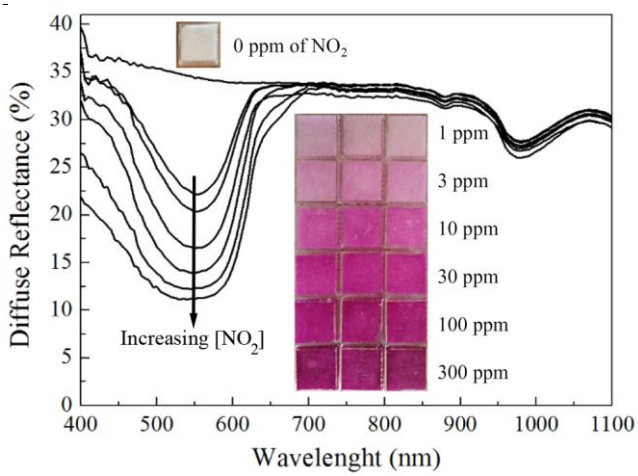

Figure 2. UV-vis diffuse reflectance of the soaked pads with GS reagent exposed to different NO_2 concentrations and the corresponding images of the colors developed (insets, 3 replicas per concentration).

$$\langle \mathrm{RGB} \rangle = Mean(\langle \mathrm{R} \rangle, \langle \mathrm{G} \rangle, \langle \mathrm{B} \rangle) \quad (4)$$

was used. Figure 3.a shows the spectral response $D(\lambda)$ of the R,G,B sensor used, together with the emission spectrum $I(\lambda)$ of the white LEDs used to illuminate the sensor pads. Therefore, combining this data with the reflectance spectra $R(\lambda)$at different NO_2 concentrations presented in Figure 2, a set of simulated ⟨R⟩, ⟨G⟩,⟨B⟩ and ⟨RGB⟩signals were calculated using eq.(3) and eq.(4).

Figure 3.b shows a comparison between the simulated ⟨R⟩, ⟨G⟩, ⟨B⟩ and ⟨RGB⟩ signals with a reference method: the intensity of the absorption peaks of the $R(\lambda)$ spectra in Figure 2, calculated as the difference with respect the blank sample at the central wavelength of the absorption band (540 nm). These latter values are the usual measurement method in color-based analytical chemistry[13]. Clearly, both procedures lead to the same qualitative trends, with quantitative differences that can be attributed to the optical differences in the two systems used for measurement. Of course, the most reliable reflected color signal is the one corresponding to the ⟨G⟩ channel, due to the matching of the green-pass filter of the G detector with the 540 *nm* absorption band of the GS-indicator. Anyhow, this suggests that any of the ⟨R⟩, ⟨G⟩, ⟨B⟩ or ⟨RGB⟩ signals from a conventional color sensor can be used to monitor the color changes in our NO_2 sensing pads.

A Model for the Color Response

In order to understand how the experimental parameters affect the color measurements, we developed an analytic model for the development of the color response in a non-reversible dye.

According to the Griess-Saltzman-type reaction chain presented in eq.(2), each indicator molecule IND_{White}acquires its colored state $\mathrm{IND}_{\mathrm{Colored}}$as a result of the capture

of the NO_2 molecules in air in the indicator solutions. The overall process can be expressed into the following simplified reaction:

$$2\,NO_{2\,air} + IND_{White} \rightarrow IND_{Colored} \quad (5)$$

This is a non-reversible process that consumes the available indicator molecules in the white state. Considering a 1st order reaction in $[IND_W]$ and an *n-th* order reaction in $[NO_{2\ air}]$ (NO_2 involves a multi-step reaction such as hydrolyzation[14] and diazotization[15]) the process can be modeled by the following set of equations:

$$\begin{cases} -\frac{d[IND_W]}{dt} = k \cdot [NO_{2\,air}]^n \cdot [IND_W] \\ [IND_W] = [IND_W]_{t=0} - [IND_C] \end{cases} \quad (6)$$

The first one stablishes that the rate (k is the rate constant) at which the white indicator molecules are consumed. The second equation sets a boundary condition to the number of indicator molecules, being all of them white before the exposure to NO_2 in air ($[IND_W]_{t=0}$). No further constrained is imposed on the availability of NO_2 in air, as it is assumed to be unlimited (i.e. the ambient being an infinite reservoir of this reagent). Combining both equations, the following differential equation rules the development of colored indicator molecules ($[IND_C]$) in presence of NO_2 in air:

$$\frac{d[IND_C]}{dt} = k \cdot [NO_{2\,air}]^n \cdot ([IND_W]_{t=0} - [IND_C]) \quad (7)$$

and has thee following analytic solution

$$[IND_C](t) = [IND_W]_{t=o} + ([IND_C]_{t=0} - [IND_W]_{t=o}) \cdot e^{-k[NO_2]^n \cdot t} \quad (8)$$

This equation can be rewritten in terms of reflected RGB color component as follows:

$$\langle S\rangle_C(\mathrm{t}) = \langle S\rangle_C^{sat} + (\langle \mathrm{S}\rangle_W^0 - \langle S\rangle_C^{sat}) \cdot \mathrm{e}^{-k\cdot[NO_2]^n \cdot \mathrm{t}} \quad (9)$$

where $\langle S\rangle_C^{sat} = [IND_C](t = \infty)$ is the signal detected when all the indicator molecules have reacted with NO_2 and $\langle S\rangle_W^0 = [IND_C](t = 0)$ is the blank signal detected at the beginning of the experiment when all the indicator molecules are in the white state.

In all these equations, an exponential decay - from an initial state (clear, white) to a colored steady state (deep-purple) - is predicted. A very long time after initiating the exposure, all the indicator molecules are colored. This time scale in which the color saturation occurs is determined by the NO_2 concentration in air.

To validate this model, eq.(9) was fitted to all the datasets in Figure 3.b.Table 1 summarizes the results from the fittings, showing that a similar agreement with the model was found in all cases. Therefore, all four measurement strategies can be used to monitor the progress of the GS indicator reaction with NO_2. In the following we will center our analysis on ⟨RGB⟩ measurements, which are the most convenient ones to carry out and the most feasible to use in an in-field application.

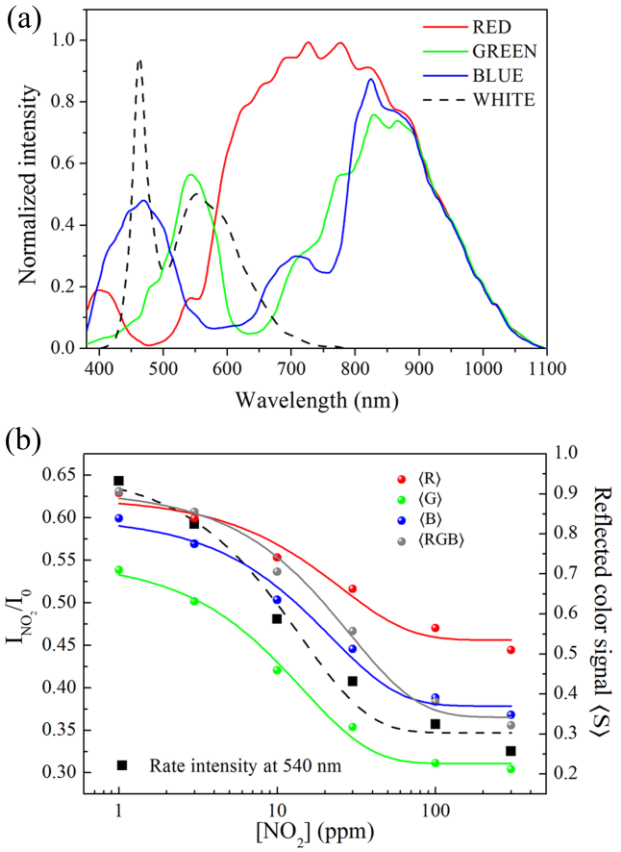

Figure 3. (a) Relative responsivity of the ⟨R⟩, ⟨G⟩ and ⟨B⟩ detectors and the emission spectra of the white LED, (b) UV-vis reflectance signal at 540 nm respect to the a blank sample (squares) and reflected color signal of the ⟨R⟩, ⟨G⟩, ⟨B⟩ mean ⟨RGB⟩ (circles) with the corresponding fitting according to eq.(9).

RGB Measurements

Exposure Time vs. Gas Concentration

Eq.(9) leads to an important conclusion: the gas concentration and the exposure time play equivalent and exchangeable roles in the development of the color change. In other words: the exposure time can be used as a design

Table 1 Fitted values from all datasets in Figure 3.b according to eq.(9).

	$\langle S\rangle_c^{sat}$	$\langle S\rangle_w^0$	$(kt)^{-1}$ ppm^{-n}	r^2
⟨R⟩	0.35	0.89	25.26	0.95
⟨G⟩	0.23	0.74	14.47	0.98
⟨B⟩	0.37	0.84	21.73	0.97
⟨RGB⟩	0.34	0.91	28.71	0.98
UV-vis	0.31	0.66	14.05	0.97

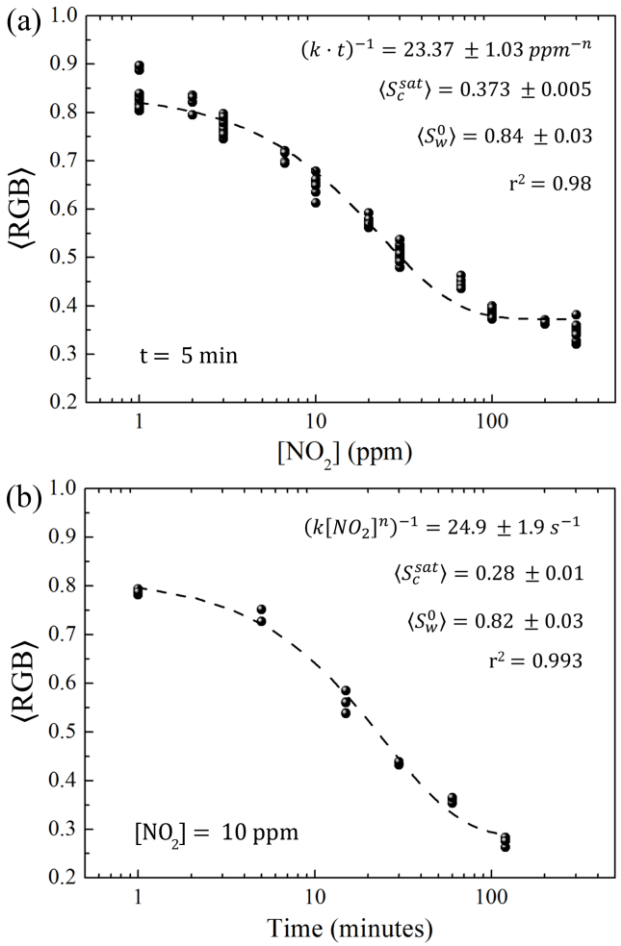

Figure 4. (a) ⟨RGB⟩ signals acquired at constant exposure time (5 min) with different NO_2 concentrations and (b) at constant concentration (10 ppm) with different exposure times. The corresponding fitting curves and values according to eq.(9) are also shown.

parameter to target different concentration ranges.

To corroborate this fact, two sets of experiments at constant concentration and at constant exposure time,werecarried out. Figure 4 shows the ⟨RGB⟩ signals acquired after 5 minutes of exposure to different NO_2 concentrations (Figure 4.a), and after increasing exposure times at a constant concentration of 10 ppm of NO_2 (Figure 4.b). The data were fitted to eq.(9), showing an excellent match in both cases: at constant exposure time and at constant $[NO_2]$ concentration. This result further supports the validity of the proposed model.

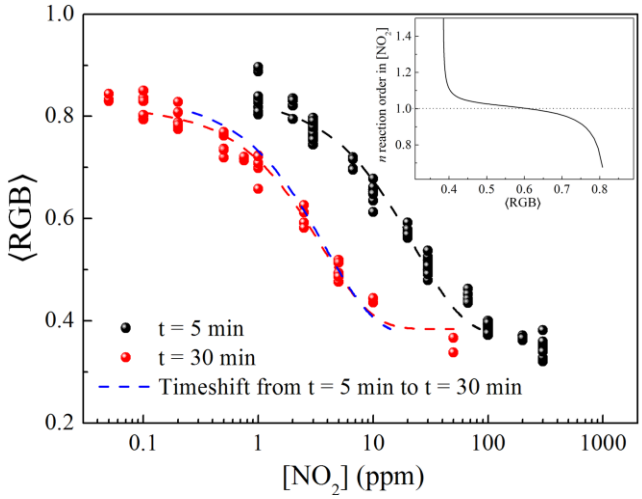

Figure 5. ⟨RGB⟩ signal for t = 5 min and t = 30 min exposure times and the corresponding fittings. Time-shifted calibration curve from t = 5 min to t = 30 min according to eq.(12). Reaction order *n* for $[NO_2]$ plot as a function of ⟨RGB⟩ signal according to eq.(11) (inset).

The dispersion of the measurements are higher at short exposure times and in the low concentration regime; because under these conditions, clearer purple shades reflect larger amounts of light, that are close to the sensor saturation range.

Optimization of the NO_2 Concentration Range

From the previous result it follows that the detection range of $[NO_2]$ can be arbitrarily extended solely by controlling the exposure time (i.e. for low detection range, larger times and vice versa). To demonstrate this, two experiments using different NO_2 concentrations and different exposure times were carried out (Figure 5). In a first set of experiments, the samples were exposed for 5 min to NO_2 concentrations ranging from 1 to 300 ppm. Then, a second set of experiments was carried out, exposing now the pads for 30 minutes to NO_2 concentrations from 50 ppb to 50 ppm. These values were selected toobtaina similar dynamic range in the ⟨RGB⟩ signal values.

Clearly, a similar color change trend was observed, with good agreement with the model (Table 2). Again, the dispersion and deviation from the fitting curve is higher in the range ends, where both the saturation and detection limits of the detectors limitthe resolution of the color sensor.

Table 2 Fitted values from datasets in Figure 5.

	$[NO_2]$ range (ppm)	$\langle RGB \rangle_W^0$	$\langle RGB \rangle_C^{sat}$	$(k \cdot t)^{-1}$ (ppm^{-n})	r^2
t = 5 min	1 – 300	0.84 ± 0.03	0.373 ± 0.005	23.37 ± 1.03	0.97
t = 30 min	0.05 – 50	0.82 ± 0.03	0.38 ± 0.01	3.6 ± 0.3	0.98

Therefore, the exposure time can be used as a parameter to tune the dynamic color range for a specific span of NO_2 concentrations. In our experiments, we could show that this span extended over four orders of magnitude, but there is no reason to think that this could not be extended further, provided that the waiting times were acceptable.

However, to know in advance the amount of time needed to target a certain range of concentrations, we need to know the exact relationship between concentration and exposure time. This means elucidating the reaction order of [NO_2] (i.e. the *n* exponent).

In order to obtain the *n* value, we considered an arbitrary pair of [NO_2] concentrations with the same ⟨S⟩ value (both values were extracted from the fitting curves):

$$\langle RGB\rangle_i([NO_2]_i, t_1 = 5\ min) = \langle RGB\rangle_i([NO_2]_i, t_2 = 30\ min)$$

If we consider that $\langle RGB\rangle^0_{W\,t=5} = \langle RGB\rangle^0_{W\,t=30}$ and $\langle RGB\rangle^{sat}_{C\ t=5} = \langle RGB\rangle^{sat}_{C\ t=30}$ (from Table 2), then:

$$[NO_2]_i^{\,n} \cdot t_1 = [NO_2]_i^{\,n} \cdot t_2 \ , \qquad (10)$$

and thus

$$n = \frac{\ln\frac{t_2}{t_1}}{\ln[NO_2]_i - \ln[NO_2]_i} \quad . \qquad (11)$$

The calculated *n* for all [NO_2] pairs with the same ⟨RGB⟩ signal extracted from the fittings are plotted in the inset of Figure 5. According to these results, the reaction order *n* is around 1, for ⟨RGB⟩ values between 0.4 and 0.8 and deviates at the range ends because of the asymptotic character of the model. Thus, we can assume that the order of the reaction in [NO_2] is approximately 1 in the central range of responses.

From a practical point of view, this means that a calibration curve (acquired at a convenient range of [NO_2] concentrations) can be easily translated to other concentration ranges, using the following relationship:

$$[NO_2]_1 \cdot t_1 = [NO_2]_2 \cdot t_2 \qquad (12)$$

In other words: the concertation-time product is a constant of a sensor pad system. To illustrate this, Figure 5 (blue line) shows an example of this procedure: the calibration curve for t = 5 min has been time-shifted to an exposure time of 30 min according to eq.(12). Clearly, this time-shifted calibration curve is perfectly usable at lower concentrations with the extended exposure time.

In summary, all this demonstrates that the proposed model successfully predicts the colorimetric response of our sensor pads and that the exposure time can be effectively used as a design parameter to adjust the response of the pads to the desired range of concentrations. This principle could be further extended, to higher and lower concentrations but unfortunately these experiments were not possible in our present experimental setup.

Specificity and Cross Interference

First, experiments with different humidity (from 0% to 100% RH)and oxygen (from 0% to 21%) backgroundconcentrationsdemonstrated that the GS reagent in our configuration was completely insensitive tovariations of these common species in air.No effects due to water in air were expected, because the pads are always soaking wet with the reagent aqueous solution. In case of oxygen, the GS reaction relies solely on the presence of nitrite ions in solution coming from the dissolution of NO_2 in water.

Later, to demonstrate the specificity of the method, pairs of equivalent pads were exposed for 30 minutes to different interfering gases blended with clean dry SA, with 1 ppm of NO_2 in SA, and with 5 ppm of NO_2 in SA. The results show (Figure 6) that the color responses were completely insensitive to the presence of any of the interfering gases used, demonstrating the specificity of the method towards NO_2.

To further demonstrate the robustness of the method, other samples were exposed to mixtures of 3 interfering gases, in addition of 0, 1, and 5 ppm of NO_2 in SA observing no difference in the colors obtained (see Figure S1 in

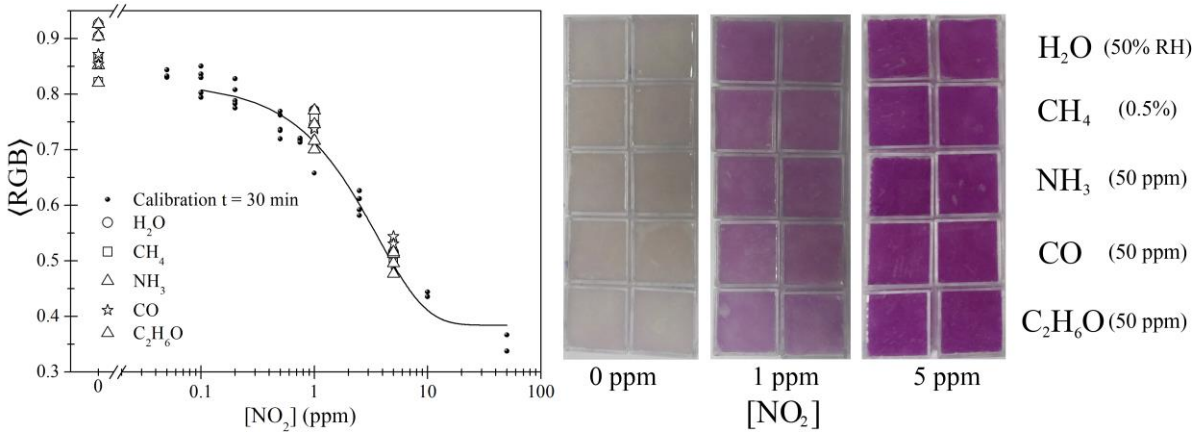

Figure 6. (Right) ⟨RGB⟩ signals for 0, 1 and 5 ppm of [NO_2] with different interfering gases (void symbols) and (left) the corresponding color development. Calibration curve for t = 30 min exposure time (filled symbols).

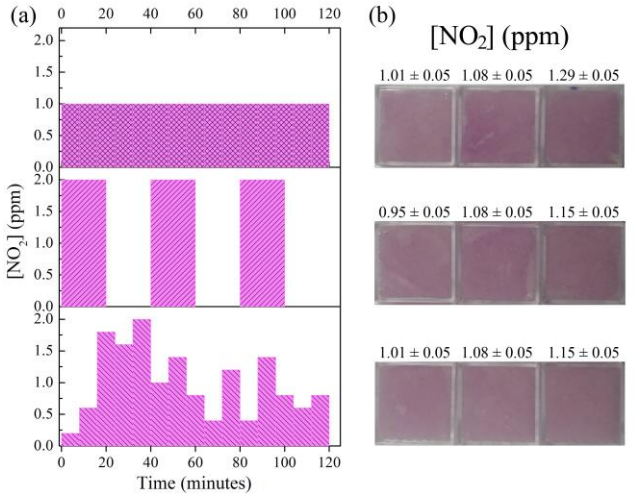

Figure 7. (a) 3 different 1 ppm average concentration sequences applied for 120 min: constant (top), 50% duty cycle (middle) and random (bottom). (b) Color development and predicted concentration in ppm from a calibration curve time-shifted from both t = 5 and t = 30 min exposure time.

Supporting Information).

Therefore, the method is robust and preservesits high specificity and low cross interference properties expected in a Griess-Saltzman-type method, but with a much more convenient form factor. Particularly relevant is the immunity to moisture, due to the abundant presence of water in the wet pads. This is not the case of other fully dry approaches[13].

Operation as Dosimeter

The fact that the Griess-Saltzman-type reactions are non-reversible makes them suitable for a dosimeter type operation. In these applications, the relevant parameter is the average gas concentration at which the sample has been exposed. This is particularly interesting with gases whose exposure limits are regulated as a maximum concentration averaged for a certain period of time. This is the case of NO_2, for which the Air Quality Standards of the European Commission dictates a concentration limit of 0.2 ppb for 1 hour period[16].

To demonstrate this mode of operation, several pads were exposed to varying sequences of NO_2 for 120 minutes. In all cases, the mean concentration of NO_2 was 1 ppm. Figure 7 shows the gas sequences used, and the color changes observed in the pads. All of them developed the same color change, corresponding to an average concentration of 1 ppm, which were determined using the calibration curve obtainedfor exposure times of 5 and 30 minutes from Figure 5, time-shifted to 120 minutes according to eq.(12) (see also Figure S2 in supporting information). The accuracy of the system is remarkable considering that the calibration curve used for predicting the average concentration had an exposure time 24-fold lower than (in the case of 5 minutes curve) the experimental exposure time.

Conclusions

We have presented a convenient method to implement a Griess-Saltzman-type reaction for the colorimetric detection of NO_2. Our soaked sensor pads are single-use devices, easy to fabricate, very cheap and can be stored for a long time, preserving their sensing properties. Their response is characterized by a high specificity towards NO_2andresponse times fast enough for ambient monitoring applications.

Their measurement can be carried out with standard RGB sensors, such as the ones found in smartphones, without significantly loosing sensing performance if compared to other, more complex and bulky, measurement systems.

We have proposed an analytic model for the color changes developed in the pads that successfully predict and match with the observations. We have shown that it can be used to tailor the response of the pads to the desired range of NO_2 concentrations, and we have demonstrated that the same pads can be used to detect NO_2 in concentrations ranging from 50 ppb to 300 ppm. We also proved that only one single calibration curve is needed, relying on the exchangeable role of NO_2 concentration and exposure time characteristic of the proposed model.

Finally, the operation of the pads as NO_2 dosimeters has also been tested, opening the door to a very promising application in the field of safety monitoring at work.

ASSOCIATED CONTENT

Supporting Information. Mixture of up to three interfering gases and calibration curve for t = 30 minutes. This material is available free of charge via the Internet at http://pubs.acs.org.

AUTHOR INFORMATION

Corresponding Author

* Cristian Fàbrega, cfabrega@el.ub.edu.

Author Contributions

The manuscript was written through contributions of all authors. All authors have given approval to the final version of the manuscript.

ACKNOWLEDGMENT

The research leading to these results has received funding from the European Research Council under the European Union's Seventh Framework Program (FP/2007-2013)/ERC Grant Agreement n. 336917 and the H2020 Framework Program ERC Grant Agreement n. 727297. J.D.Prades acknowledges the support from the Serra Húnter Program. The technical support of Dr. Daniel Sanz, from the Facility of Chemistry of the Universitat de Barcelona, is thankfully acknowledged.

REFERENCES

(1) Sudalma, S.; Purwanto, P.; Santoso, L. W. The Effect of SO2

and NO_2 from Transportation and Stationary Emissions Sources to SO_4 And NO_3 In Rain Water in Semarang. *Procedia Environ. Sci.***2015**, *23*, 247–252.

(2) Chen, T.-M.; Kuschner, W. G.; Gokhale, J.; Shofer, S. Outdoor Air Pollution: Nitrogen Dioxide, Sulfur Dioxide, and Carbon Monoxide Health Effects. *Am. J. Med. Sci.***2007**, *333*, 249–256.

(3) Cooney, R. V.; Ross, P. D.; Bartolini, G. L.; Ramseyer, J. N-Nitrosoamine and N-Nitroamine Formation: Factors Influencing the Aqueous Reactions of Nitrogen Dioxide with Morpholine. *Environ. Sci. Technol.***1987**, *21*, 77–83.

(4) Riess, J. Nox: How Nitrogen Oxides Affect the Way We Live and Breathe. *US Environ. Prot. Agency, Off. Air Qual. Plan. Stand.***1998**.

(5) Oregon Waste Systems, Inc. v. Department of Environmental Quality of Ore. *US*, 1994, *511*, 93.

(6) Privett, B. J.; Shin, J. H.; Schoenfisch, M. H. Electrochemical Sensors. *Anal. Chem.***2008**, *80*, 4499–4517.

(7) Liu, Y.; Parisi, J.; Sun, X.; Lei, Y. Solid-State Gas Sensors for High Temperature Applications ? A Review. *J. Mater. Chem. A***2014**, *2*, 9919–9943.

(8) Rakow, N. a; Suslick, K. S. A Colorimetric Sensor Array for Odour Visualization. *Nature***2000**, *406*, 710–713.

(9) Brochure, Dräger AG. „Das Labor hinter Glas. Dräger-Röhrchen" https://www.draeger.com/Products/Content/labor-hinter-glas-roehrchen-br-9046078-de.pdf (accessed Apr 10, 2017).

(10) Saltzman, B. E. Colorimetric Microdetermination of Nitrogen Dioxide in Atmosphere. *Anal. Chem.***1954**, *26*, 1949–1955.

(11) Fisher, G. E.; Becknell, D. E. Saltzman Method for Determination of Low Concentrations of Oxides of Nitrogen in Automotive Exhaust. *Anal. Chem.***1972**, *44*, 863–866.

(12) Passaretti Filho, J.; da Silveira Petruci, J. F.; Cardoso, A. A. Development of a Simple Method for Determination of NO_2 in Air Using Digital Scanner Images. *Talanta***2015**, *140*, 73–80.

(13) Izumi, K.; Utiyama, M.; Maruo, Y. Y. Colorimetric NOx Sensor Based on a Porous Glass-Based NO_2 Sensing Chip and a Permanganate Oxidizer. *Sensors Actuators, B Chem.***2015**, *216*, 128–133.

(14) Finlayson-Pitts, B. J.; Wingen, L. M.; Sumner, A. L.; Syomin, D.; Ramazan, K. A.; Schrems, O.; Miller, H.; Miskovic, P.; Nozaki, A.; Tsuzuki, T.; *et al.* The Heterogeneous Hydrolysis of NO_2 in Laboratory Systems and in Outdoor and Indoor Atmospheres: An Integrated Mechanism. *Phys. Chem. Chem. Phys.***2003**, *5*, 223–242.

(15) Lyshkow, N. A. A Rapid and Sensitive Colorimetric Reagent for Nitrogen Dioxide in Air. *J. Air Pollut. Control Assoc.***1965**, *15*, 481–484.

(16) Standards - Air Quality - Environment - European Commission http://ec.europa.eu/environment/air/quality/standards.htm (accessed Jun 28, 2017).

For TOC only

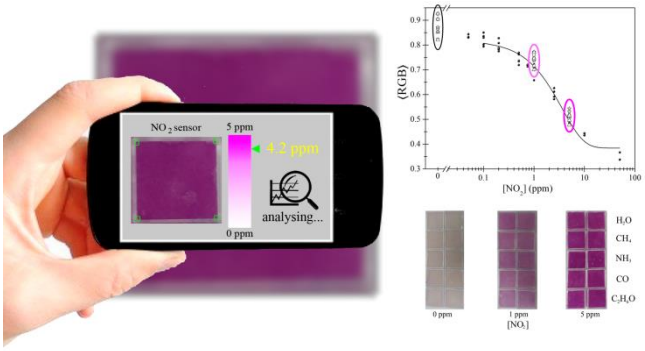
NO 2 sensor
5 ppm
4.2 ppm
analysing...
0 ppm
(RGB)
[NO2] (ppm)
H2O
CH4
NH3
CO
C2H5O
0 ppm
1 ppm
5 ppm
[NO2]